Hyper Velocity Acceleration by a Pulsed Coilgun Using Traveling Magnetic Field

Katsumi Masugata, *Member, IEEE*

***Abstract*— A method is proposed to accelerate a projectile by using a propagating magnetic field in a pulse transmission network. The acceleration is shown to be limited by the ohmic heating of the projectile and the obtainable final velocity is estimated. The final velocity is shown to be enhanced by a factor of two by cooling the projectile down to 77 K from 300 K. The final velocity is described as a function of the projectile radius and shown that more than 10 km/s is obtainable by using the Al projectile of radius more than 0.9 cm. From the result of circuit simulation, magnetic field is confirmed to propagate in the pulse transmission network.**

***Index Terms*— Coil gun, electromagnetic launcher, traveling magnetic field.**

I. Introduction

An electromagnetic launcher system can accelerate a projectile to a hyper velocity of more than 5 km/s. A railgun has been considered to be a promising candidate to obtain such a velocity. However, in the railgun, the rails are strongly damaged due to the current flow between the rails and the plasma armature, which make a multishot operation difficult. In addition, coupling inductance is very low in the railgun and very-low-impedance power supply is necessary to obtain an efficient acceleration. In the coilgun [1]–[4], armature current is induced inductively in the metallic armature and a sliding contact is not necessary, which makes possible the damage-free acceleration. In addition, coupling impedance of the coil is relatively high and it is adjustable by changing a coil parameter, which makes possible the efficient coupling without using a special power supply. However, the coilgun has been considered suitable for the acceleration of a low velocity heavy projectile and it is not considered for hyper velocity acceleration.

In this paper, a consideration of hyper velocity acceleration of projectile by a pulsed coilgun is described. A limit of the maximum velocity is estimated and shows the possibility to apply for hyper-velocity acceleration. A coilgun using a pulsed-traveling magnetic field is proposed to obtain the hyper velocity.

II. Design and Evaluation of Pulsed Coilgun

Fig. 1 shows the basic principle of the pulsed coilgun. The coilgun consists of driving coils and a cylindrical projectile of conductive material. When a driving coil is excited by a pulsed current, diamagnetic current is produced in the projectile, which produces a repulsive force. By the sequentially triggering of the coils, the projectile is repetitively accelerated in each coil.

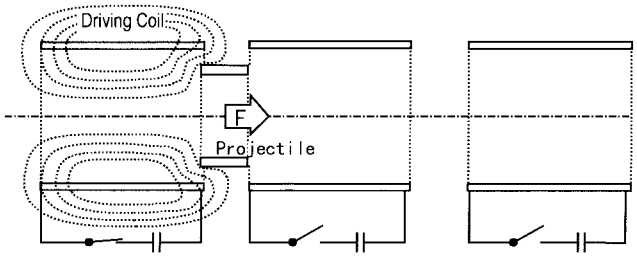

Fig. 1. Basic principle of the pulsed coilgun.

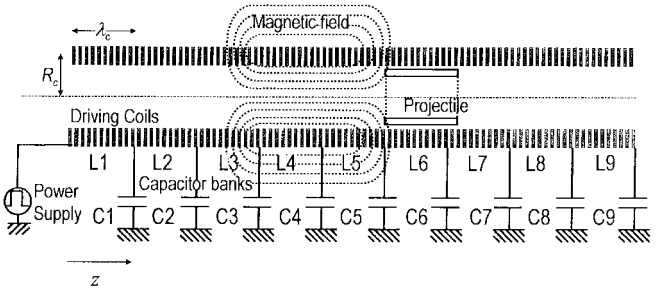

Fig. 2. Conceptual drawing of the acceleration of the projectile in the pulse transmission network.

In the coilgun, the acceleration occurs when the projectile is passing around the exits of the driving coils and the acceleration is intermittent. In addition, large number of driving coils are utilized that are triggered synchronously with the position of the projectile. The synchronization is not easy and the efficiency is reduced since switching of many switches is necessary. If a driving coil is moving with a projectile continuous acceleration is expected, which can be virtually realized by using a traveling magnetic field in a pulse transmission network.

Fig. 2 shows the conceptual drawing of the acceleration of a projectile in a pulse transmission network. In the system a network of inductors (L) and capacitors (C) is utilized and by applying a pulsed voltage to the first coil (L_1), a pulsed traveling magnetic field is produced.

In the following, the principle of the acceleration is described to estimate the limitation of final velocity. From the estimation, final velocity is described as a function of the radius of the projectile.

Manuscript received March 3, 1997; revised July 28, 1997.

The author is with the Nagaoka University of Technology, Nagaoka, Niigata 940-21, Japan.

Publisher Item Identifier S 0018-9464(97)07758-3.

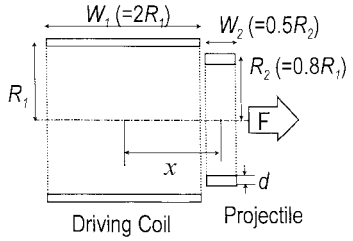

Fig. 3. Single stage pulsed induction accelerator configuration to estimate the magnetic force.

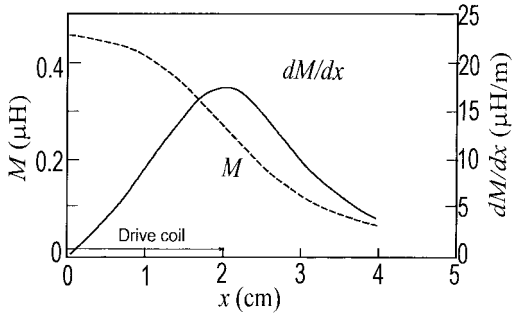

Fig. 4. Calculated curves of M and dM/dx plotted against x. Here, $R_1 = 2$ cm and $N_1 = 24$ are assumed.

A. Estimation of Electromagnetic Force

Fig. 3 shows the single-stage pulsed-induction accelerator configuration to estimate the magnetic force. Here, a driving coil of radius R_1, width W_1 and a cylindrical projectile of radius R_2, width W_2 are placed on an axis. Here, x is the center-to-center distance between the driving coil and the projectile. In this case, the repulsive force (F) is described as follows [2]:

$$F = \frac{dM}{dx} I_c \cdot I_p \tag{1}$$

where M is the mutual inductance between the driving coil and the projectile I_c and I_p are the driving coil current and a projectile current, respectively. Assuming that current density distributions in the driving coil and in the projectile are uniform and that the thickness of the drive coil and the projectile (d) is sufficiently thin to use a thin coil approximation, M can be described as follows:

$$M = \frac{\mu\pi R_1^2 R_2^2 N_1 N_2}{2W_1} \cdot \left[\frac{2}{R_1^2}\left(\frac{l_2}{d_2} - \frac{l_1}{d_1}\right) - \frac{R_2^2}{4}\left(\frac{l_1}{d_1^5} - \frac{l_2}{d_1^5}\right)\left(3 - \frac{W_2^2}{R_2^2}\right)\right]$$

where

$$l_1 = x - \frac{W_1}{2}, \quad l_2 = x + \frac{W_1}{2},$$
$$d_1 = \sqrt{l_1^2 + R_1^2}, \quad d_2 = \sqrt{l_2^2 + R_1^2}. \tag{2}$$

Here, N_1 and N_2 are the turn number of the driving coil and the projectile, respectively. To calculate the repulsive force and evaluate the dependence on the radius of the projectile, the aspect ratio of the coil and the projectile is fixed as described in the figure ($W_1 = 2R_1$, $R_2 = 0.8R_1$, $W_2 = 0.5R_2 = 0.4R_1$).

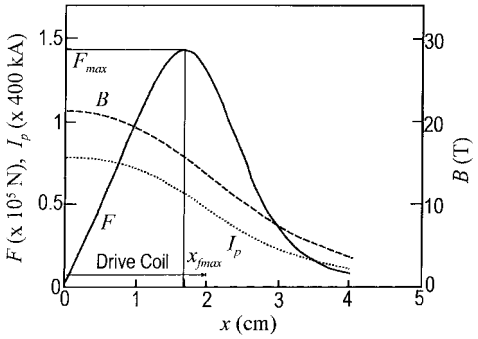

Fig. 5. Distribution of F, I_p, and B when $I_c = 40$ kA, plotted against x. B is calculated for the case without the projectile.

Since the projectile is expected to act as a perfect diamagnetic magnet for the duration of $\tau = L_p/R_p$, the resistance can be ignored for the duration. Here, R_p is the one turn resistance of the projectile and L_p is the self inductance of the projectile described by

$$L_p = 10^{-7}\lambda \frac{(2\pi R_2 N_2)^2}{W_2} \tag{3}$$

where λ is the Nagaoka's coefficient [5] and it is 0.37 in this case. In the case, I_p is calculated by the following:

$$I_p = I_c \frac{M}{L_p}. \tag{4}$$

Fig. 4 shows the example of the calculated curve of M against x for the case of $R_1 = 2$ cm and $N_1 = 24$ (in the case $W_1 = 4$ cm, $R_2 = 1.6$ cm, $W_2 = 0.8$ cm, $N_2 = 1$). As seen in the figure, M decreases with increasing x and dM/dx has a peak at $x \approx 2$ cm (that corresponds to the exit of the driving coil). In the parameter, the self inductance of the driving coil (L_c) and L_p is evaluated to be 3.1 μH and 58 nH, respectively.

Fig. 5 shows the distribution of repulsive force (F) with I_p when $I_c = 40$ kA. A magnetic field distribution on the axis when the projectile is absent is also described as the reference. As seen in the figure, 22 T of magnetic field is produced in the center of the driving coil. As the stress limit of specially designed pulsed coil is around 50 T, the value seems to be conservative. Maximum repulsive force ($F_{\max}$) of 1.4×10^5 N is obtained at $x = x_{f_{\max}} = 1.7$ cm, where I_p is evaluated to be 220 kA ($= I_{pf_{\max}}$). If assuming the Al projectile of $d = 3.2$ mm, corresponding mass (m_p) is 22.9 g and in the case acceleration (α) of 6.2×10^6 m/s^2 (6.3×10^5 G) is obtained. If the projectile is accelerated continuously in the condition, it reaches to 5 km/s in 0.81 ms in an acceleration length (or a length of the launcher) of 8 m.

Fig. 6 shows the dependence of $F_{\max}$ and $I_{pf_{\max}}$ as a function of R_2. Here, I_c is assumed to increase linearly with R_1 to keep the magnetic field on the center of the coil to be $\approx$22 T. As seen in the figure, $I_{pf_{\max}}$ linearly increases with increasing R_2 whereas $F_{\max}$ is proportional to the square of R_2.

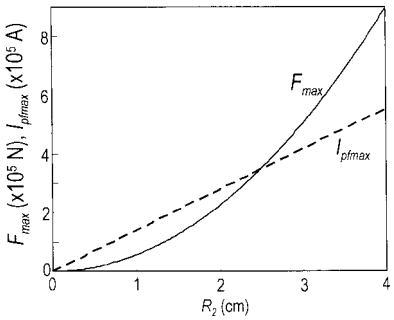

Fig. 6. Dependence of $F_{\max}$ and $I_{pf_{\max}}$ on R_2. Here, I_c is assumed to be proportional to R_1 to keep the magnetic field on the center of the coil to be $\approx$22 T.

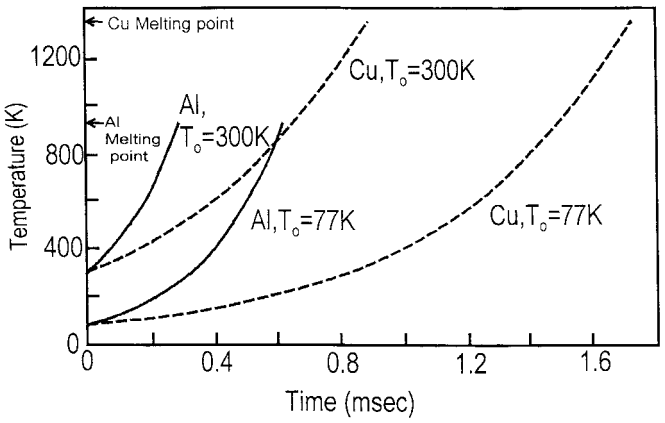

Fig. 7. Calculated temperature of the projectile when current density (J) of 10^{10} A/m^2 (1 MA/cm^2) is assumed.

B. Estimation of Acceleration Time

In the coil gun, the obtainable final velocity is limited by a heat up of the projectile. That is, the projectile is ohmicly heated and if it reaches the melting point it melts and collapses and is no longer accelerated. The temperature of the projectile (T) is calculated by the following:

$$dT = \frac{J^2\rho}{\kappa} \tag{5}$$

where J is the current density and ρ and κ are the resistivity and specific heat of the projectile, respectively, both of which are temperature dependent. Fig. 7 shows the calculated temperature of the projectile when current density $J = 10^{10}$ A/m^2 (1 MA/cm^2) is assumed. Copper and aluminum projectiles are assumed with initial temperature (T_0) of 77 and 300 K. The melting points are 1357.7 and 933.6 K for Cu and Al, respectively. As seen in the figure, heating speed (gradient of T) increases with increasing T due to the increase of ρ as the heating. The durations to reach the melting points (τ) are found to be elongated by a factor two in both materials by reducing T_0. The duration corresponds to the maximum acceleration time of the projectile.

Here, considering that the heating speed is inversely proportional to J^2, a normalized acceleration time (τ_n) is introduced, which is the product of τ with J^2. Fig. 8 shows the dependence of τ_n plotted against T_0. As seen in the figure, τ_n has a strong dependence on T_0 and can be enhanced by reducing T_0.

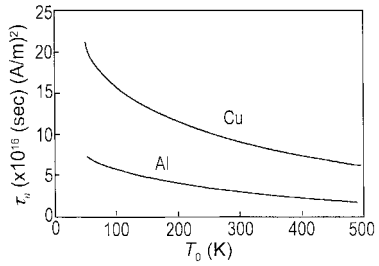

Fig. 8. Dependence of normalized acceleration time τ_n plotted against T_0.

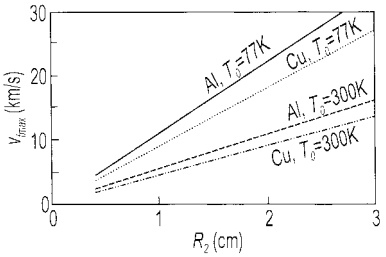

Fig. 9. Obtainable final velocity of Al and Cu projectiles plotted against R_2 when the d is assumed to be $0.2R_2$.

C. Final Velocity

The possible final velocity (v_{final}) of the projectile is calculated from α and τ as

$$v_{\text{final}} = \alpha\tau = \frac{F\tau}{m_p} = \frac{F_{\max}\tau}{m_p} \tag{6}$$

where, m_p is the mass of the projectile. For a fixed aspect ratio with fixed thickness of the projectile (d), v_{final} is described as a function of R_2. Fig. 9 shows the example of v_{final} for Al and Cu projectile plotted against R_2 when d is $0.2R_2$ (which corresponds to 0.16 R_1). As seen in the figure, v_{final} linearly increases with R_2. Higher velocity is obtained in Al projectile as compared to Cu due to the lower mass density of Al, even though the smaller value of τ_n. Final velocity of more than 10 km/s is expected for projectiles of $R_2 > 0.9$ cm, and >1.1 cm when using Al and Cu projectile, respectively, with $T_0 =$ 77 K.

In the fixed aspect ratio, α and τ can be described as functions of R_1 and d as shown in the following:

$$\alpha = \frac{F_{\max}}{m_p} \propto \frac{1}{d}, \text{ (since } m_p \approx \rho_m 2\pi \cdot R_2 \cdot W_2 \cdot d \propto R_1^2 \cdot d, \quad F_{\max} \propto R_1^2)$$

$$\tau \propto \frac{1}{J_{\max}^2} \propto \left(\frac{W_2 d}{I_{p_{\max}}}\right)^2 \propto \frac{R_1^2 d^2}{R_1^2} \propto d^2. \tag{7}$$

From the relation, we see that v_{final} is proportional to d and, hence, thick projectile is preferable to obtain a higher velocity. However, since thin coil approximation is utilized in the above calculation with uniform current density, the error increases for a thick projectile and the dependence on d is not evaluated.

D. Circuit Simulation

The propagation of magnetic field in the pulse-transmission network shown in Fig. 2 is confirmed by the computer simulation. Here, considering the unit coil of radius $R_1 = 2$ cm,

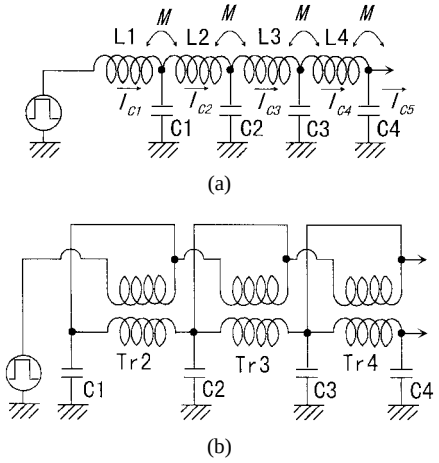

Fig. 10. Circuit models of the coilgun.

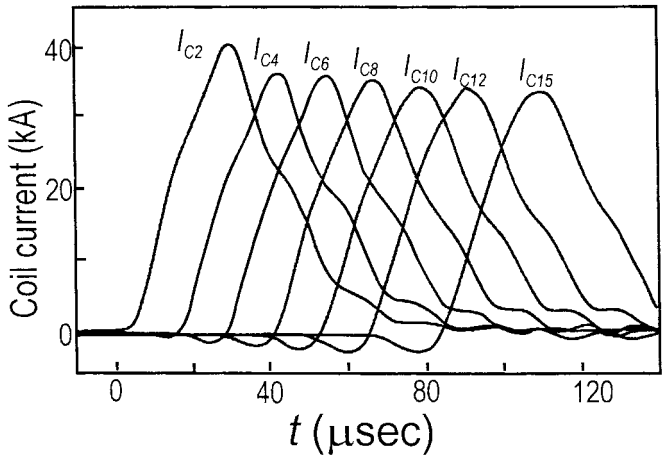

Fig. 11. Current waveforms of each coil obtained by the simulation.

width $\lambda_c = 2$ cm, and turn number $N_1 = 12$, (2) and (3) are again utilized to evaluate a self inductance (L_s) and a mutual inductance of the coils (M). Here, mutual inductances between the coils side by side and that between the coil and the coil next, but one are evaluated to be 1.89 and 0.46 μH, respectively, the latter was ignored for simplicity. L_s is calculated to be 6.4 μH. The interaction with the projectile is not considered.

Fig. 10(a) shows the circuit model for the coilgun system. Here, a pair of the coils placing side by side is considered as a $1:1$ transformer of coupling coefficient $(k) = 0.308$, and the inductance of primary and secondary turns $(L_1, L_2) = 6.4$ μF. Then the circuit is rewritten as Fig. 10(b). In the simulation, the capacitors ($C_1, C_2, C_3, \cdots$) are assumed to be 10 μH and a pulsed of voltage of 64 kV, duration 25 μs, rise and fall time 5 μs is applied to the circuit.

Fig. 11 shows current waveforms of each coil obtained by the simulation. As seen in the figure, similar waveforms of peak current >30 kA, duration 31 μs full width at half maximum (FWHM) are obtained with delay time in a unit of the coil of 6.3 μs. A negative pre-pulse is glowing as the propagation of the pulse, which is caused by the mutual

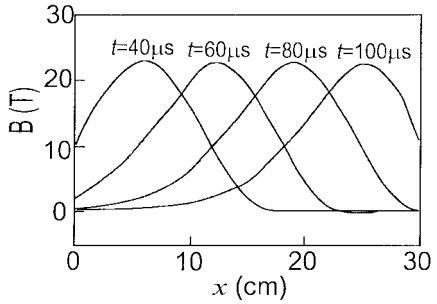

Fig. 12. Magnetic field distribution on the axis at each timing obtained by the simulation.

inductance. Considering the width of the coils (2 cm), the propagation velocity is calculated to be 3.9 km/s. The propagating velocity can be changed by changing the circuit parameters. For example, the propagation velocity is evaluated to be 4.4 km/s when replacing the capacitors of 10 μF by capacitors of 5 μF.

Fig. 12 shows the magnetic field distribution on the axis at each timing. As seen in the figure, magnetic field of peak strength ($\approx$23 T, width $\approx$11 cm (FWHM) is propagating downstream keeping the profile. From the simulation, the propagation of magnetic field in the pulse transmission network was confirmed and by using the propagating magnetic field the projectile is expected to be accelerated.

In the model, interaction of the magnetic field with a projectile is not considered for simplicity. However, in the acceleration process, energy of magnetic field is converted to the kinetic energy of the projectile and as a result the pulse energy (duration and the peak current) decreases as the acceleration. To compensate the reduction, multistages of coils are necessary to be utilized in the real system, each stage is powered separately.

III. Conclusion

A method is proposed to accelerate a projectile by using a propagating magnetic field in a pulse-transmission network. The acceleration is shown to be limited by the ohmic heating of the projectile and the obtainable final velocity is estimated. The final velocity is shown to be enhanced by a factor of two by cooling the projectile down to 77 K from 300 K. The final velocity is described as a function of the projectile radius and shown that more than 10 km/s is obtainable by using the Al projectile of radius more than 0.9 cm. From the result of circuit simulation, magnetic field is confirmed to propagate in the pulse transmission network.

The results are preliminary and may be optimistic since very simple models are utilized. However, it was sufficient to introduce the concept of the acceleration. In the next stage of the study, more exact simulation should be utilized to design the realistic system. In the simulation, two-dimensional (2-D) electromagnetic field solver, including eddy current effect, is utilized with 2-D equation of motion. From the simulation, acceleration efficiency, electromagnetic stress in the coil and in the projectile, the temperature distribution in the projectile, or the stability will be evaluated.

ACKNOWLEDGMENT

The author expresses his gratitude to Prof. K. Yatsui for frequent, stimulating, and helpful discussions.

REFERENCES

[1] S. Kim, H. Jung, and S. Hahn, "An optimal design of capacitor driven coilgun," *IEEE Trans. Magn.*, vol. 30, pp. 207–211, 1994.
[2] H. Kolm and P. Mongeau, "Basic principles of coaxial launch technology," *IEEE Trans. Magn.*, vol. MAG-20, pp. 227–230, 1984.
[3] K. MacKinney and P. Mongeau, "Multiple stage pulsed induction acceleration," *IEEE Trans. Magn.*, vol. MAG-20, pp. 239–242, 1984.
[4] D. G. Elliott, "Traveling wave induction launchers," *IEEE Trans. Magn.*, vol. 25, pp. 159–163, 1989.
[5] Tabulated in *Radio Engineers Handbook.* New York: McGraw-Hill, 1943.

Katsumi Masugata (M'95) received the B.E. degree from Osaka University, Japan, in 1978, the M.E. degree from Nagaoka University of Technology, Japan, in 1982, and the Ph.D. degree from Osaka University, in 1988.

Since 1982, he has been with the Department of Electrical Engineering, Nagaoka University of Technology, where he is now an Associate Professor. His research interests have included pulse-power technology, generation and diagnostic of high-power pulsed-particle beams, and high-current arc plasma.